Supporting Information

Predicting Keto-Enol Equilibrium from Combining UV/Visible Absorption Spectroscopy with Quantum Chemical Calculations of Vibronic Structures for Many Excited States - A Study Case on Salicylideneanilines

Freddy ZUTTERMAN,[a] Orian LOUANT,[a] Gabriel MERCIER,[b] Tom LEYSSENS,[b] and Benoît CHAMPAGNE[a,*]

[a.] *Laboratoire de Chimie Théorique, Unité de Chimie-Physique Théorique et Structurale, Namur Institute of Structured Matter, Université de Namur, rue de Bruxelles, 61, B-5000 Namur (BELGIUM).*

[b] *Institute of Condensed Matter and Nanosciences, Université Catholique de Louvain, 1 Place Louis Pasteur, B-1348 Louvain-La-Neuve (BELGIUM)*

benoit.champagne@unamur.be

Details on the theoretical and computational methods.

Geometry optimization of the salicylideneanilines (SA's) were carried out at the Møller-Plesset Second-Order (MP2) level of approximation as well as using density functional theory (DFT) with the B3LYP-35 [A] and M06 [B] exchange-correlation (XC) functionals, together with the 6-311+G(d,p) basis set in both cases. The B3LYP-35 XC functional corresponds to the B3LYP functional where 35% of HF exchange are used instead of the 20% of the original one [A]. This functional was shown to be reliable for predicting vibronic structure of UV/visible absorption spectra as well for simulating resonant Raman spectra. The "tight" optimization criterion of Gaussian [C] was employed together with the

"`ultrafine`" grid of integration (99 radial shells with 590 angular points per shell) for the DFT calculations. All structures correspond to minima on the potential energy surfaces, as evidenced by the real values of the vibrational frequencies. These were employed together with the rotational constants to calculate the partition functions, and thereof the Gibbs free enthalpies. Solvent effects were taken into account using the polarizable continuum model (PCM) in its integral equation formalism (IEF) [D]. Acetonitrile and ethanol, respectively, were selected for **1** and **2** because experimental data are available in these solvents for these two SA's.

To simulate the absorption spectra and their vibronic structure we followed the procedure described in two of our recent publications [E, F]. The B3LYP-35/6-311+G(d,p) level of approximation in combination with IEF-PCM (solvent = acetonitrile/ethanol) has been adopted for both ground state (DFT) and excited state (TDDFT) characterizations. In order to account for anharmonicity effects as well as for the limitations of the methods a multiplicative factor f = 0.94 has been used to scale down the harmonic vibrational frequencies [G]. Contrary to quinacridone and FP chromophore models, the UV/visible spectra contain bands originating from more than one electronic excitation. The dominant ones were included in the simulation of the vibronic structure. TDDFT calculations afforded the 20 lowest-energy excited states. Those with an excitation energy below 4.96 eV (above 250 nm) and an oscillator strength larger than 0.01 were kept. To evaluate the vibronic structure, the gradient method was adopted in combination with the TDDFT method of non-equilibrium solvation. So, the geometry of the excited state is not fully optimized. It is approximated from the knowledge of gradients of the excitation energy along the various normal coordinates at the ground state equilibrium geometry. While reliable, this method is easy to employ and usually feasible for all situations, including when the optimized geometries of the ground and excited states are very different or when there are many excited states in the same energy range, which renders their individual geometry optimizations difficult.

The FC_ellipse program calculates the vibronic structure within the Franck-Condon approximation. The program allows selecting a reduced set of vibronic excitations, which

are defined by the vibrational quantum numbers vector, [$\nu = (\nu_1, \nu_2, \ldots, \nu_{3N-6})$], with $\nu_p = 0, 1, 2, \ldots$ the vibrational quantum number of mode p and 3N-6 the number of vibrational normal modes. For each system, a few low-frequency (< 100 cm^{-1}) vibrational normal modes with large Huang-Rhys (HR) factors have been discarded. They are associated with strongly anharmonic modes, which mostly broaden and smooth the vibronic structure. The HR factors describe the difference of geometry between the electronic ground and excited states along the different ground-state normal coordinates. Then, FC_ellipse can couple a maximum of 10 normal modes (level = 10), *i.e.* 10 different vibrations can be excited ($\nu_p \neq 0$). In practice, the level parameter is varied to control the convergence of the sum of the FC factors, which tends to 1. As shown further, level = 6 is sufficient. At last, the combinations of vibrational quantum numbers are controlled by an ellipsoid-like expression:

$$\sum_{p=1}^{3N-6} \left(\frac{\nu_p}{R_p} \right)^2 \leq 1$$

where $R_p = g.HR_p^{1/2}$ and g is set to 9. This functional form comes from the observation that the largest FC factor is obtained when ν_p is of the order of the HR_p factor. Finally, when simulating the spectra, only those FC factors larger than the FCMin threshold are kept. This approach to predict the characteristics of the absorption spectra of anils model chromophores presents similarities to those applied over the last decade to evaluate excitation energies, oscillator strengths, and vibronic structures of a broad set of chromophores.

Spectra were simulated with a homemade code, which applies peak broadening to all vibronic transitions. Gaussian peak shapes were used with a typical full width at half of the maximum (FWHM) of 0.1 eV. This FWHM = 0.1 eV value allows visualizing the vibronic structure whereas a larger value would be more appropriate for a closer match with the experimental spectra (*e.g.* Figure S2/Bottom, FWHM = 0.15 eV). Peak broadening is needed in order to empirically account for several factors that are not included in the theoretical treatment. Since geometry optimizations were not carried out for the excited states it is impossible to position the simulated absorption spectra with vibronic structure

on the energy scale, as this necessitates the global 0-0 excitation energy to be known. The UV-from-QM code arbitrarily uses the vertical excitation energy as the onset of the spectrum because the 0-0 excitation energy is unknown. Moreover, in the plotted spectra we applied an energy shift to the entire spectrum. This energy shift was chosen such that the absorption maxima of the simulated and experimental spectra coincide. For compounds **1**-**4**, the energy shifts amount to -0.510 eV, -0.510 eV, -0.425 eV, and -0.415 eV, respectively.

Complementary calculations of the excitation energies and oscillator strengths were carried out at the CC2 level [H] using the def2-TZVP basis set. These were performed using the Turbomole 6.0 package [I] for isolated molecules (no solvent effects) using the TDDFT/B3LYP-35/6-311+G(d,p)/IEF-PCM(acetonitrile) optimized geometries. Values of the $\|T2\|$ diagnostic for the excitation energies of the enol form are between 8.37 and 9.77% while these values range between 8.53 and 11.76% for the keto form.

Details on the synthesis and UV/vis absorption measurements.

Materials: Solvents and starting materials for synthesis were all purchased and used as such. Product codes are given in brackets. From Accros Organics: ortho-vanilin (150-586); from TCI: 2-hydroxy-1-naphthaldehyde (708-06-5); from U.C.B. s.a.: aniline (1163-494); and from VWR Chemicals: acetonitrile (200-835-2) and ethanol (200-578-6).

Synthesis of 1: 5 mmol of 2-hydroxy-1-naphthaldehyde was dissolved in 10 ml MeCN at 50°C in a 50 ml beaker. 5 mmol of aniline were added to the solution and the solution was stirred manually for 5 minutes. Yellow solid started to appear after 10 minutes and the mixture was let to evaporate overnight. The solid was dried at 45°C for 48h and used as such (yield: 99%, purity: 97%).

Synthesis of 3 (See Fig. S2): 10 mmol of ortho-vanilin was added to 10 mmol of aniline in a 50 ml beaker and the reaction started immediately. 5 ml of pure ethanol was added in order to complete the reaction and the solution was stirred manually for 10 minutes and let evaporate overnight. The solid was dried at 45°C for 48h and used as such (yield: 99%, purity: 99%).

UV/vis absorption spectrum: 21.91 mg of **1** were dissolved in 20 ml of pure MeCN. The spectrum of this $4.4 \cdot 10^{-3}$ M solution was then recorded at room temperature on a Shimadzu UV-1700 PharmaSpec spectrophotometer from 800 to 200 nm. The same equipment was used for **3**. In that case 23.0 mg of **3** was dissolved in 20 ml of pure MeCN ($5.0 \cdot 10^{-3}$ M). The spectrum of **2** has been taken from Figure 1 of Ref. [J]. It has been recorded in ethanol. To allow comparison with calculations, this spectrum was digitalized using the WebPlotDigitizer tool [K]. The same procedure was employed for the experimental spectrum of **4**, which was taken from Figure 2 of Ref. [L].

Table S1. Vertical transition energies, wavelengths, and oscillator strengths (in parentheses) of **1** and **2** in their enol and keto forms as evaluated at the TDDFT/B3LYP-35/6-311+G(d,p) on B3LYP-35/6-311+G(d,p) optimized geometries. All calculations were carried out by accounting for solvent (acetonitrile for **1** and ethanol for **2**) effects using IEF-PCM.

Enol form		keto form	
1			
Calc.	**Exp.**	**Calc.**	**Exp.**
#1, 3.56 eV, 348.0 nm (0.580)	3.31 eV, 375 nm	#1, 3.19 eV, 388.1 nm (0.551)	2.86 eV, 433 nm
#2, 4.21 eV, 294.6 nm (0.142)		#2, 3.92 eV, 316.0 nm (0.131)	
#3, 4.37 eV, 283.6 nm (0.011)		#3, 3.95 eV, 313.9 nm (0.071)	
#4, 4.61 eV, 269.0 nm (0.013)		#4, 4.34 eV, 285.8 nm (0.165)	
		#5, 4.68 eV, 265.2 nm (0.074)	
2			
Calc.	**Exp.** [a]	**Calc.**	**Exp.**
#1 3.54 eV, 350.5 nm (0.457)		#1 3.08 eV, 402.1 nm (0.567)	2.75 eV, 451 nm
#2 4.12 eV, 300.9 nm (0.234)		#3 4.13 eV, 300.4 nm (0.222)	
#3 4.38 eV, 283.3 nm (0.298)	4.00 eV, 310 nm	#4 4.28 eV, 289.4 nm (0.580)	
#4 4.78 eV, 259.4 nm (0.593)		#6 4.82 eV, 257.3 nm (0.167)	
#5 4.87 eV, 254.7 nm (0.047)		#7 4.95 eV, 250.3 nm (0.061)	
		#8 5.10 eV, 243.1 nm (0.088)	

[a] in the case of the enol form of **2**, the lowest-energy bands are hidden by those of the dominant keto form, preventing comparisons. On the other hand, the band peaking at 310 nm is related to 3rd and 4th excited states of the enol form as well as the 4th and 6th excited states of the keto form.
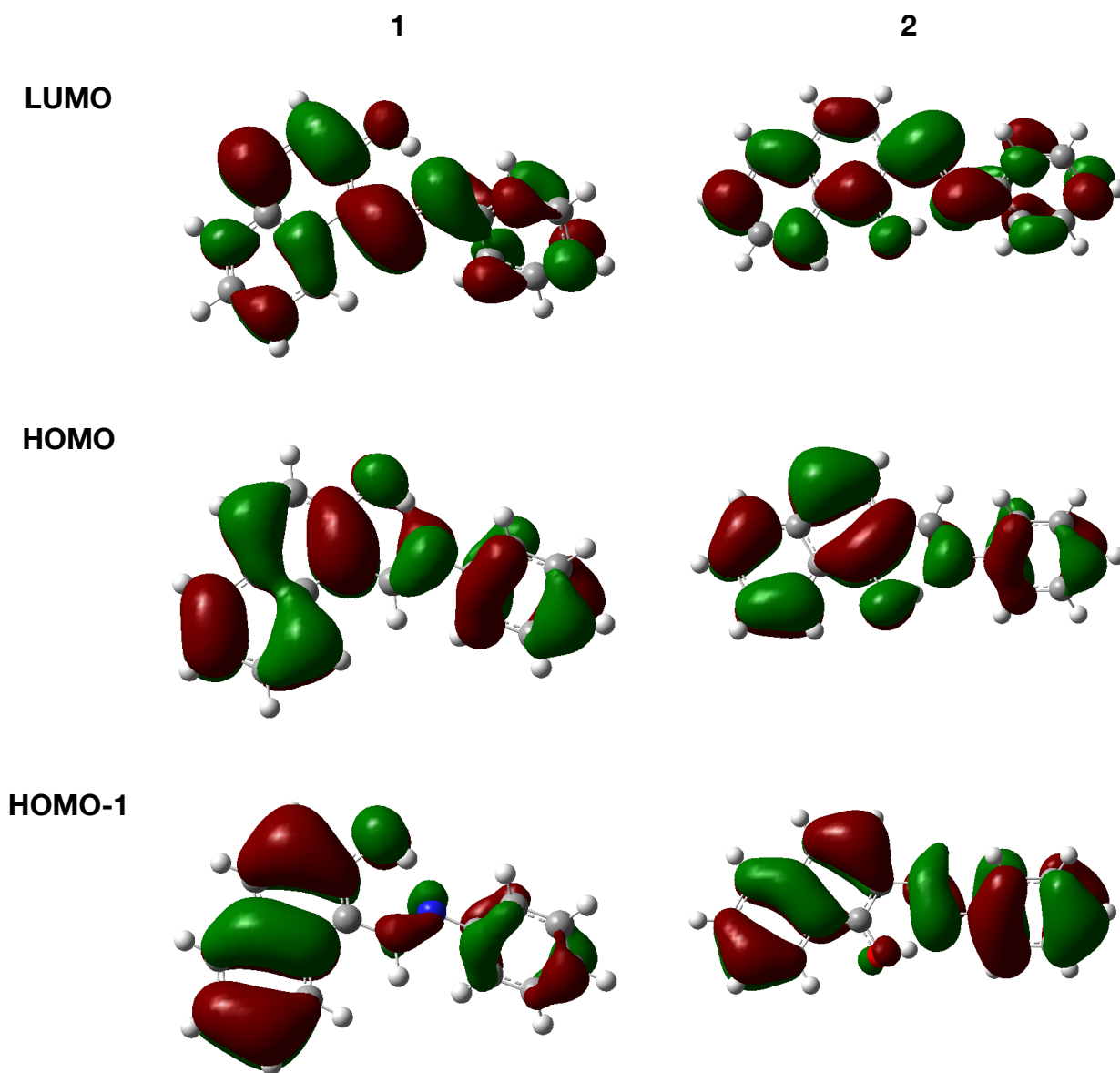
1   **2**

LUMO

HOMO

HOMO-1

Figure S1. HOMO-1, HOMO, and LUMO of **1** and **2** as determined at the B3LYP-35/6-311+G(d,p)/IEF-PCM(acetonitrile/ethanol) on geometries optimized at the same levels.
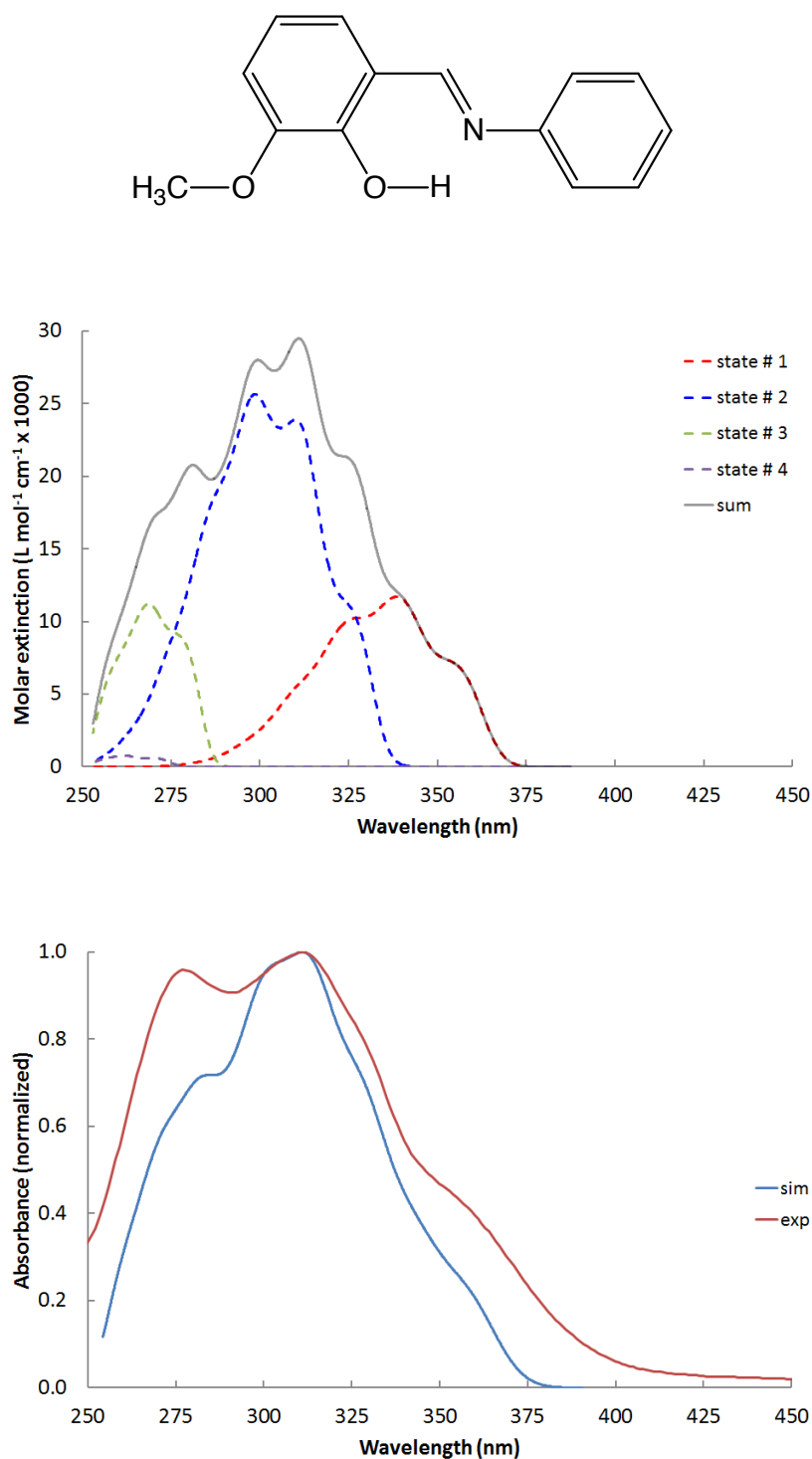
Figure S2. Structure (Top) and UV/visible absorption spectra (Middle and Bottom) of SA **3** in its enol form; Middle) Decomposition of the simulated absorption spectrum [at the TDDFT/B3LYP-35/6-311+G(d,p)/IEF-PCM(cyclohexane) level] into its lowest-energy excited states contributions with FWHM = 0.1 eV; Bottom) Comparison between experimental and simulated spectra after increasing the FWHM to 0.15 eV. The experimental spectrum was obtained in cyclohexane.
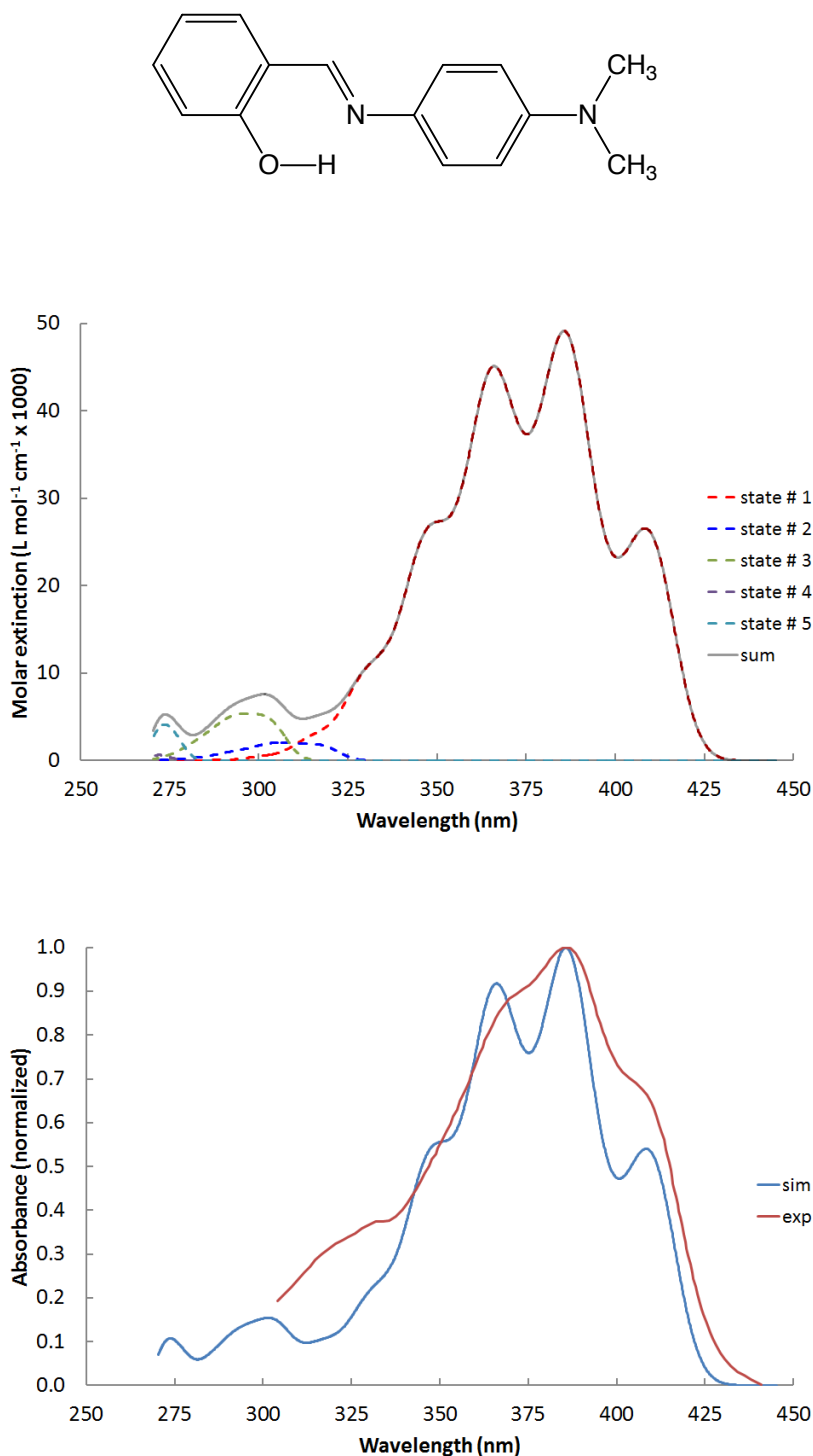
Figure S3. Structure (Top) and UV/visible absorption spectra (Middle and Bottom) of SA **4** in its enol form; Middle) Decomposition of the simulated absorption spectrum [at the TDDFT/B3LYP-35/6-311+G(d,p)/IEF-PCM(cyclohexane) level] into its lowest-energy excited states contributions with FWHM = 0.1 eV; Bottom) Comparison between experimental and simulated spectra. The experimental spectrum was taken from Vargas, V.; Amigo, L. A study of the Tautomers of *N*-Salicylidene-*p*-X-Aniline Compounds in Methanol, *J. Chem. Soc., Perkin Trans.* **2001**, *2*, 1124-1129.
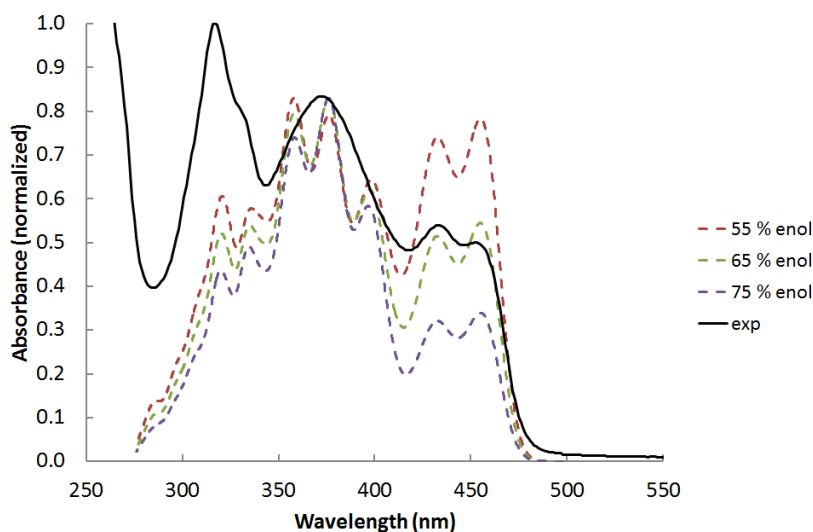
Figure S4: Simulated spectrum of **1** for different keto:enol abundance ratios (25:75, 35:65, and 45:55) in comparison with experiment. The simulated spectrum has been obtained at the TDDFT/B3LYP-35/6-311+G(d,p)/IEF-PCM(acetonitrile) level.
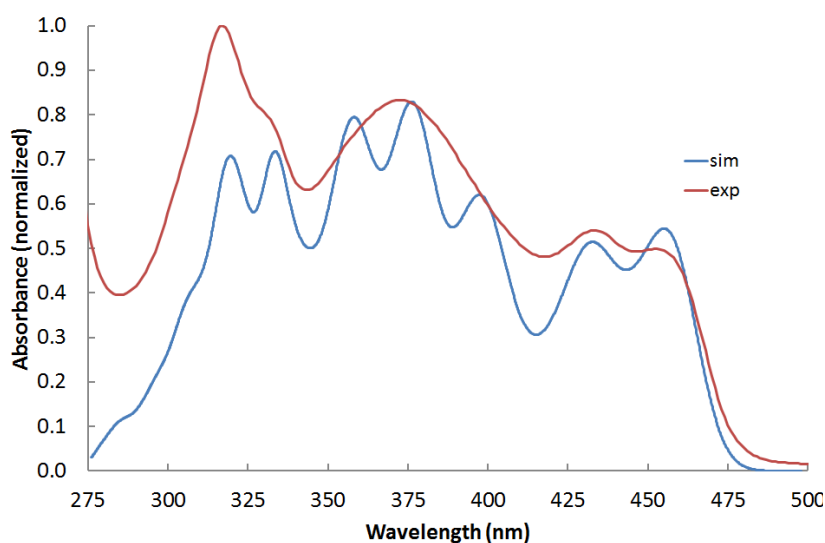

Figure S5: Simulated spectrum of **1** for a 35:65 keto:enol mixture in comparison with experiment. The simulated spectrum has been obtained at the TDDFT/B3LYP-35/6-311+G(d,p)/IEF-PCM(acetonitrile) level but the oscillator strength of the third transition of the enol form has been scaled by taking into account the corresponding CC2 values.

REFERENCES

[A]   Guthmuller, J.; Champagne, B. Time-Dependent Density Functional Theory Investigation of the Resonance Raman Properties of the Julolidinemalononitrile Push-Pull Chromophore in Various Solvent, *J. Chem. Phys.* **2007**, *127*, 164507.

[B]   Zhao, Y.; Truhlar, D. G. The M06 Suite of Density Functionals for Main Group Thermochemistry, Thermochemical Kinetics, Noncovalent Interactions, Excited States, and Transition Elements: Two New Functionals and Systematic Testing of Four M06-Class Functionals and 12 Other Functionals, *Theor. Chem. Acc.* **2008**, *120*, 215–241.

[C]   Frisch, M. J.; Trucks, G. W.; Schlegel, H. B.; Scuseria, G. E.; Robb, M. A.; Cheeseman, J. R.; Scalmani, G.; Barone, V.; Mennucci, B.; Petersson, G. A., et al. *Gaussian 09*, Revision D01; Gaussian, Inc.: Wallingford, CT, 2009.

[D]   Tomasi, J.; Mennucci, B.; Cammi, R. Quantum Mechanical Continuum Solvation Models. *Chem. Rev*. **2005**, *105*, 2999-3094.

[E]   Champagne, B.; Liégeois, V.; Zutterman, F. Pigment Violet 19 – A Test Case to Define a Simple Method to Simulate the Vibronic Structure of Absorption Spectra of Organic Pigments and Dyes in Solution, *Photochem. Photobiol. Sci.* **2015**, *14*, 444-456.

[F]   Zutterman, F.; Liégeois, V.; Champagne, B., Simulation of the UV/vis Absorption Spectra of Fluorescent Protein Chromophore Models, *ChemPhotoChem* **2017**, *1*, 281-296.

[G]   Merrick, J. P.; Moran, D.; Radom, L. An Evaluation of Harmonic Vibrational Frequency Scale Factors *J. Phys. Chem. A* **2007**, *111*, 11683–11700.

[H]   Christiansen, O.; Koch, H.; Jørgensen, P. The Second-Order Approximate Coupled Cluster Singles and Doubles Model CC2. *Chem. Phys. Lett.,* 1995, 243, 409–418.

[I]   TURBOMOLE V6.0.2 2009, a Development of University of Karlsruhe and Forschungszentrum Karlsruhe GmbH, 1989-2007, TURBOMOLE GmbH, Since 2007.

[J]   Fabian, W.M.F.; Antonov, L.; Nedeltcheva, D.; Kamounah, F.S.; Taylor, P.T. Tautomerism in Hydroxynaphthaldehyde Anils and Azo Analogues: a Combined Experimental and Computational Study, *J. Phys. Chem. A*, **2004**, 108, 7603-7612.

[K]   Rohatgi, A., WebPlotDigitizer 4.0, Austin, TX, USA.

[L]   Vargas, V.; Amigo, L. A study of the Tautomers of *N*-Salicylidene-*p*-X-Aniline Compounds in Methanol, *J. Chem. Soc., Perkin Trans.* **2001**, *2*, 1124-1129.